



Antecedence of the Yarlung–Siang–Brahmaputra River, eastern Himalaya

Karl A. Lang*, Katharine W. Huntington

Department of Earth and Space Sciences and Quaternary Research Center, Johnson Hall, Rm. 070, Box 351310, University of Washington, Box 351310, Seattle, WA 98195, USA

ARTICLE INFO

Article history:

Received 17 January 2014

Received in revised form 11 April 2014

Accepted 12 April 2014

Available online 13 May 2014

Editor: T.M. Harrison

Keywords:

Detrital zircon U–Pb geochronology

River capture

Arunachal Pradesh Himalaya

Siwalik Group

Tsangpo Gorge

Eastern Himalayan Syntaxis

ABSTRACT

At the eastern terminus of the Himalayan orogen, distortion and capture of southeast Asian drainage basins reflects regional patterns of crustal strain due to the indentation of the Indian Plate into Eurasia. After flowing eastward >1000 km along the southern margin of Tibet, the Yarlung–Siang–Brahmaputra River turns abruptly southward through the eastern Himalayan syntaxis rapidly exhuming a crustal scale antiform in an impressive >2 km knickpoint. This conspicuous drainage pattern and coincidence of focused fluvial incision and rapid rock exhumation has been explained by the capture of an ancestral, high-elevation Yarlung River by headward erosion of a Himalayan tributary. However, recent observation of Tibetan detritus in Neogene foreland basin units complicates this explanation, requiring a connection from Tibet to the foreland prior to the estimated onset of rapid rock exhumation. We constrain the sedimentary provenance of foreland basin units deposited near the Brahmaputra River confluence in the eastern Himalayan foreland basin using detrital zircon U–Pb geochronology. We interpret the significant presence of Gangdese-age detritus in each foreland basin unit to indicate that connection of the Yarlung–Siang–Brahmaputra River was established during, or prior to foreland deposition in the Early Miocene. Our results indicate that connection of the Yarlung–Siang–Brahmaputra River precedes exhumation of the syntaxis, demonstrating the potential for the progressive coevolution of rock uplift and rapid erosion of the Namche Barwa massif.

© 2014 Elsevier B.V. All rights reserved.

1. Introduction

The peculiar drainage patterns of large southeast Asian rivers reflect a complex history of crustal deformation and river reorganization. For example, distortion of the upper Salween, Mekong and Yangtze rivers may be explained by warping of antecedent drainage basins (e.g. Burrard and Hayden, 1907; Brookfield, 1998; Hallet and Molnar, 2001) from collision of the eastern Indian Plate margin with the Eurasian Plate (e.g. Peltzer and Tapponier, 1988; Holt et al., 1991; Royden et al., 1997; Sol et al., 2007) beginning in the Early Eocene (Searle et al., 1987; Garzanti and Van Haver, 1988; Yin, 2006; Najman, 2006). Near the Indian indentor corner in the eastern Himalayan syntaxis (Fig. 1), locally steepened river channels (e.g. Seeber and Gornitz, 1983), barbed tributaries (e.g. Burrard and Hayden, 1907; Burchfiel et al., 2000; Clark et al., 2004) and low drainage divides within the Yarlung–Siang–Brahmaputra drainage basin provide evidence that such dis-

tortion can culminate in drainage reorganization by capture and reversal (e.g., Clark et al., 2004; Clift et al., 2006).

Of particular interest is a ~100 km reach where the Yarlung–Siang–Brahmaputra River abruptly bends southward through the eastern syntaxis after flowing eastward >1000 km along terrane boundaries (Brookfield, 1998), dropping >2 km from the Tibetan plateau between >7 km Himalayan peaks. This anomalously steep (Seeber and Gornitz, 1983) and narrow (Montgomery, 2004) reach (i.e. knickzone) known as the Tsangpo gorge, is a locus of extremely rapid and focused erosion (e.g. Finlayson et al., 2002; Finnegan et al., 2008; Stewart et al., 2008; Larsen and Montgomery, 2012) coincident with an active crustal-scale antiform, the Namche Barwa massif (Fig. 2A; e.g. Burg et al., 1997, 1998; Ding et al., 2001; Kidd et al., 2006; Quanru et al., 2009; Xu et al., 2012a). Thermochronological, geochronological and petrological analyses of metamorphic and anatetic bedrock in the core of the massif constrain rapid exhumation rates exceeding 5 km/Myr since at least the Pliocene (Burg et al., 1998; Malloy, 2004; Seward and Burg, 2008) or Late Miocene (Ding et al., 2001; Booth et al., 2009; Xu et al., 2012a), and analyses of erosional efflux further indicate that modern erosion rates are also high (e.g. Galy and France-Lanord, 2001; Singh and France-Lanord, 2002; Garzanti et al., 2004;

* Corresponding author.

E-mail addresses: karllang@uw.edu (K.A. Lang), kate1@uw.edu (K.W. Huntington).



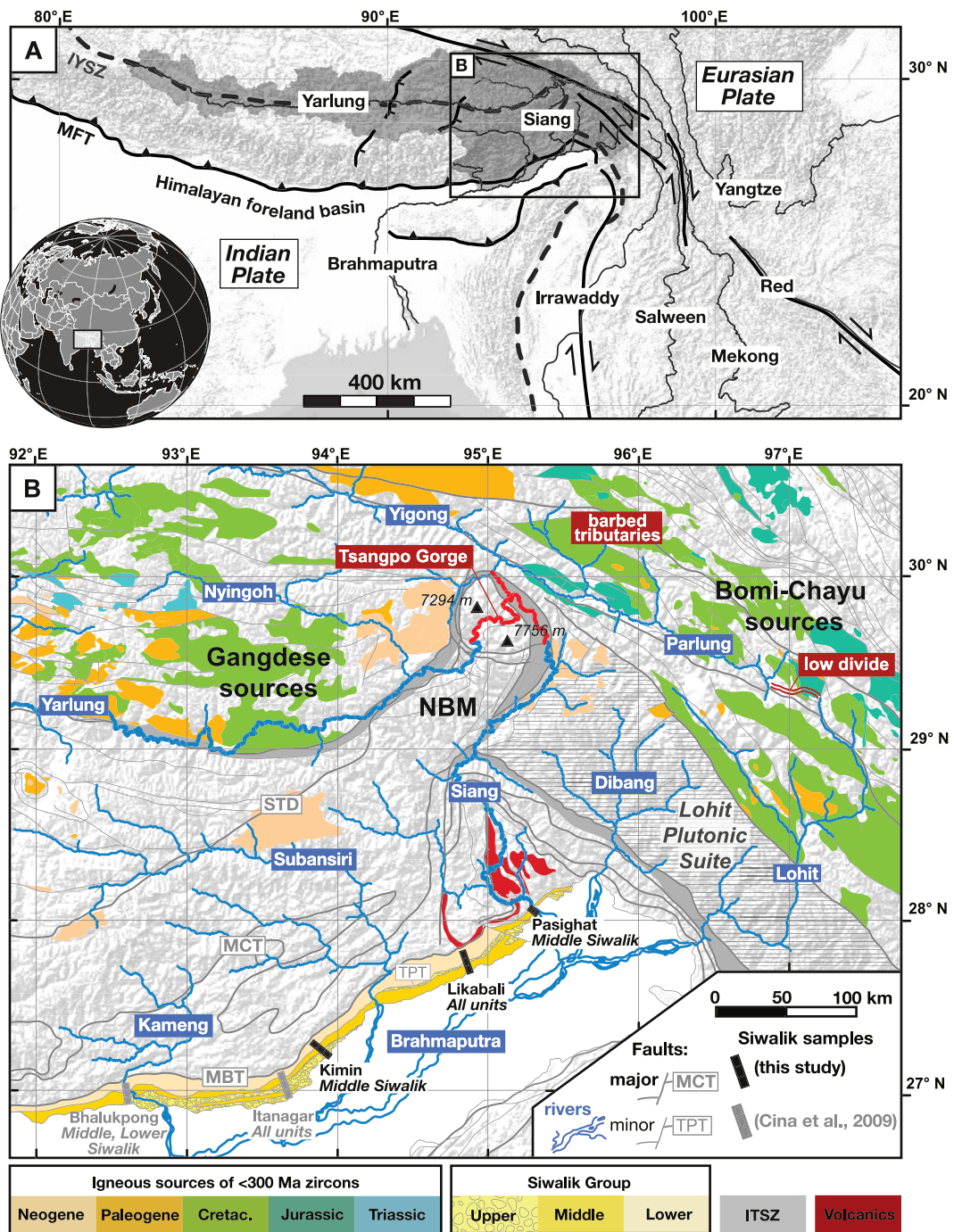


Fig. 1. Study area in the eastern Himalayan syntaxis. (A) The Yarlung River follows the Indus-Yarlung Suture Zone (IYSZ, dashed) along the southern margin of Tibet before sharply turning southward to flow through the eastern Himalayan syntaxis, becoming the Siang River prior to joining the Brahmaputra River in the eastern Himalayan foreland basin (drainage area shaded). (B) Compilation of regional geological mapping (from Armijo et al., 1989; Agarwal et al., 1991; Kidd et al., 2006; Pan et al., 2004; Acharya, 2007; Misra, 2009; Yin et al., 2010) illustrates potential source areas for <300 Ma zircons in igneous rocks north of the IYSZ and within the eastern Himalaya. We sampled Siwalik foreland basin units from three new locations (Kimin, Likabali, Pasighat) to constrain sedimentary provenance upstream of previous observations near Bhalukpong and Itanagar (Cina et al., 2009; Chirouze et al., 2013). Major tectonic features are labeled for reference: the Tipi Thrust (TPT), Main Boundary Thrust (MBT), Main Central thrust (MCT), and South Tibetan Detachment (STD).

Pik et al., 2005), potentially exceeding 10 mm/yr (Stewart et al., 2008; Enkelmann et al., 2011).

Initiation of such rapid exhumation has been explained by the capture of a high elevation, ancestral Yarlung drainage basin via headward erosion of a steep Himalayan tributary (Fig. 2B; e.g., Burrard and Hayden, 1907; Gregory and Gregory, 1925; Seeber and Gornitz, 1983; Brookfield, 1998; Clark et al., 2004). The resulting increase in drainage area and discharge to a knickzone at

the point of capture would have increased the river's erosional potential, causing the knickzone to propagate upstream in a wave of incision. However, this knickzone has not relaxed into the Tibetan plateau as predicted by a simple model of upstream propagation (Finnegan et al., 2008), but has instead remained at the margin of the Tibetan plateau in the vicinity of the Namche Barwa massif.

Alternatively, connection of the Yarlung and Siang Rivers may predate uplift of the Namche Barwa massif (e.g. Harrison et al.,

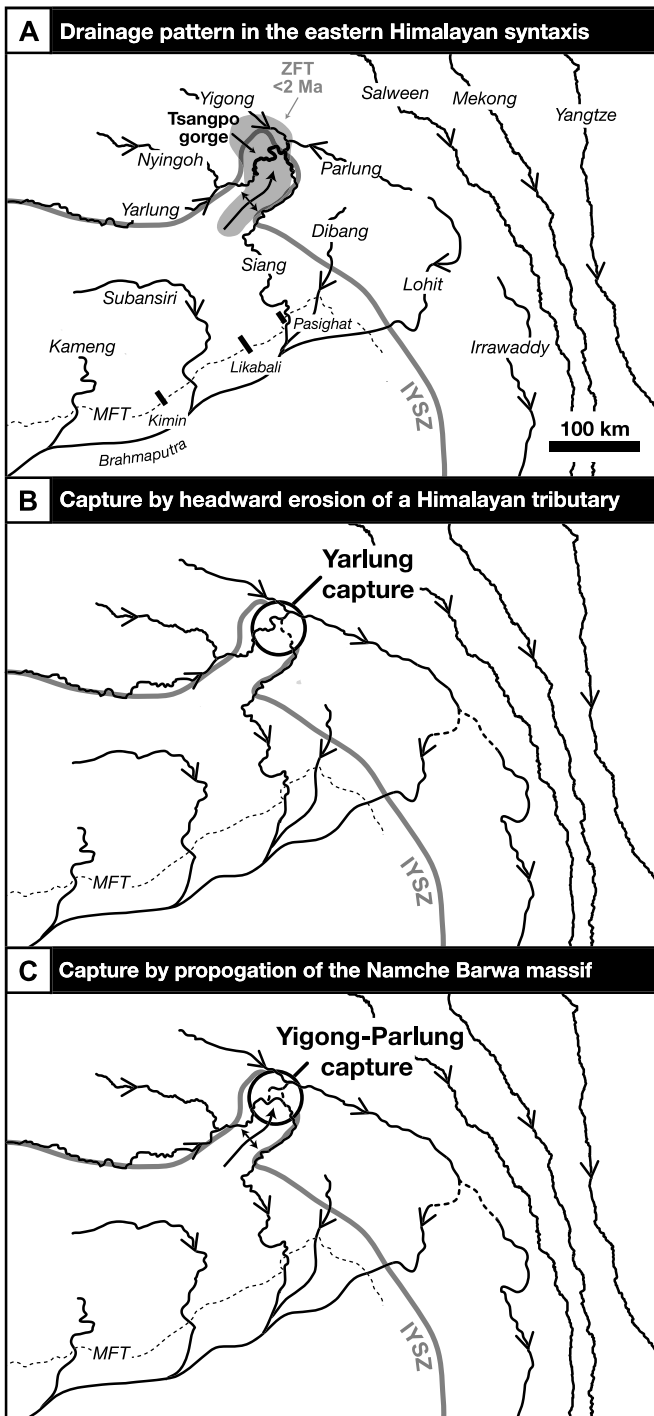


Fig. 2. Modern drainage pattern and explanations of river capture and drainage evolution. (A) The tortuous modern route of the Yarlung–Siang–Brahmaputra River across the rapidly exhuming Namche Barwa massif (defined by gray area of zircon fission-track (ZFT) cooling ages <2 Ma, Enkelmann et al., 2011). (B) Headward erosion of a Himalayan tributary may have captured an ancestral east-draining Yarlung River to initiate rapid exhumation at the capture location (e.g. Clark et al., 2004), or (C) lateral propagation of the massif may have forced an integrated Yarlung–Siang–Brahmaputra River to capture an ancestral east-draining Yigong–Parlung River (e.g. Seward and Burg, 2008).

1992; Seward and Burg, 2008), in which case the Tsangpo gorge would represent a stationary knickzone resulting from localized uplift of the massif due to lithospheric buckling (e.g. Burg et al., 1998; Burg and Podladchikov, 1999) or geometric stiffening of the indenting margin of the Indian Plate (e.g., Ehlers and Ben-

dick, 2013). Localized rock uplift will steepen the equilibrium channel profile of rivers crossing the massif, locally increasing the potential for fluvial incision (Whipple and Tucker, 1999) and it has been proposed that rapid incision of an uplifting massif may eventually lead to a thermo-mechanical feedback (e.g. Koons, 1995, 1998; Koons et al., 2013; Zeitler et al., 2001) sustaining rapid rock exhumation and explaining the locally high topography (Finlayson et al., 2002; Finnegan et al., 2008), elevated geothermal gradient (Craw et al., 2005) and antiformal structure (Koons et al., 2002; Simpson, 2004) observed in the vicinity of the Tsangpo gorge. Seward and Burg (2008) noted that if the Yarlung–Siang connection predated uplift of the massif, the geomorphic evidence for reversal of the Parlung River (e.g. barbed tributaries to the Parlung River and the low divide in Fig. 1; Burchfiel et al., 2000; Clark et al., 2004) may indicate that lateral propagation of the antiform forced the capture of an ancestral Yigong–Parlung River by the Yarlung–Siang–Brahmaputra (Fig. 2C).

In this paper, we investigate the integration of the Yarlung–Siang–Brahmaputra River with new detrital zircon U–Pb provenance constraints from sedimentary units deposited along the eastern extent of the Himalayan foreland basin. Provenance analysis allows us to constrain the timing of Yarlung–Siang–Brahmaputra integration from the proximal sedimentary record, expanding on the prior work from sedimentary sections south of the Subansiri River (Cina et al., 2009; Chirouze et al., 2013) to determine when the Yarlung and Brahmaputra Rivers connected through the Siang. We use the collective dataset to interpret the Neogene evolution of rivers draining into the eastern Himalayan foreland, placing new constraints on the relationship between fluvial incision and tectonic deformation in this dynamic region.

2. Background

2.1. Sedimentary units of the eastern Himalayan foreland basin

Our study focuses on samples from three sedimentary sections exposed in the Himalayan foothills along the margin of the eastern Himalayan foreland basin near the town of Pasighat and the villages of Likabali and Kimin (Fig. 1). Of these three sections, the two near Likabali and Pasighat are upstream of the Subansiri–Brahmaputra River confluence, and the one near Kimin is downstream of the confluence.

Beginning in the Pleistocene (Kumar, 1997; Chirouze et al., 2013), movement on the Tipi Thrust and Main Frontal Thrust has uplifted a sequence of sedimentary rocks estimated to be at least ~ 6 km (Jain et al., 1974; Agarwal et al., 1991; Chirouze et al., 2012) and as much as ~ 10 km thick (Karunakaran and Ranga Rao, 1976; Ranga Rao, 1983; Kumar, 1997). GPS data indicate that convergence across the eastern Himalaya is dominantly perpendicular to the mountain front with a maximum of 6–7 mm/yr of sinistral movement in the eastern Himalaya (see compilation in Burgess et al., 2012). If convergence was similar throughout the Neogene (e.g. Molnar and Stock, 2009), the foreland basin units exhumed at the mountain front should have originally been deposited near the orthogonal position of their present exposure.

The sedimentary rocks exposed in these sections comprise an upward-coarsening clastic sequence broadly interpreted to represent filling of a peripheral foreland basin with detritus shed from the rising Himalaya (e.g. Ranga Rao, 1983; Kumar, 1997; Najman, 2006). Three lithologically distinct units are observed within this sequence (Jain et al., 1974; Ranga Rao, 1983; Agarwal et al., 1991); progressing up-section these are: (1) alternating beds of fine grained sandstone with carbonaceous shale, followed by (2) very thickly bedded, massive and cross-bedded medium to

coarse grained sandstone with coalified logs, centimeter to meter scale calcareous nodules and gravel to cobble channel lag deposits, and (3) interbedded siltstone, sandstone, and clast supported gravel to cobble conglomerate with coarse to very coarse grained sand and silt lenses. The ages of the depositional contacts between each unit are paleontologically (Ranga Rao, 1983; Kumar, 1997) and magnetostratigraphically (Chirouze et al., 2012) constrained to ~10–11 Ma between the lower and middle units, and ~2–3 Ma between the middle and upper units.

Regional literature classifies these three units as the Dafla, Subansiri and Kimin formations, respectively (e.g. Ranga Rao, 1983; Kumar, 1997; Cina et al., 2009; Burgess et al., 2012); however, the units are loosely correlated to the Lower, Middle and Upper Siwalik units in the Western and Central Himalaya (e.g. Ranga Rao, 1983; Kumar, 1997; Najman, 2006; Chirouze et al., 2012), a terminology we adopt for consistency with the broader Himalayan literature.

Field observations from the Likabali section provide some indication of the sedimentary provenance of the units. Clast lithologies of conglomeratic beds in the Upper Siwalik unit contain variously colored quartzite (red, green, white, gray), volcanic rocks including amygdular basalt, high-grade metamorphic rocks including gneiss and schist, and dolomite (Jain et al., 1974). We observed these clast lithologies in conglomerate beds across the Upper-Middle Siwalik transition as well as in channel lag gravels within the Middle Siwalik unit, where amygdular basalt, gneiss, volcanic breccia, quartzite (red, purple, white, gray), vein quartz, and dolomite first appear. These clast lithologies are generally characteristic of Lesser Himalayan metasedimentary units in the eastern Himalaya (e.g. Singh, 1993; Kumar, 1997; Acharyya, 2007; Yin et al., 2010; Kesari, 2010), but the distinct presence of volcanic rocks suggests a specific source region from the ‘Abor volcanics’ exposed along the Siang River (e.g. Jain and Thakur, 1978; Ali et al., 2012).

Paleocurrent indicators from multiple sections in the eastern Himalaya consistently show either south or southwest paleoflow directions, indicating that source areas remained north of sample locations during deposition of this sedimentary sequence. South-directed paleocurrent indicators, have been observed in the Upper Siwalik unit from imbricate pebbles near Itanagar (Cina et al., 2009) and cobbles near Likabali (Jain et al., 1974) and Bhalukpong (Kesari, 2010). Paleocurrent indicators in the Middle Siwalik unit indicate a variable (Chirouze et al., 2013), but dominantly southwest-directed paleoflow direction as measured on cross-bedding in pebbly conglomerate lag deposits near Itanagar (Cina et al., 2009) and Bhalukpong (Kesari, 2010; Chirouze et al., 2013). A dominantly southwest-directed paleoflow is also interpreted from cross-bedding in the Lower Siwalik unit near Bhalukpong (Chirouze et al., 2013).

Collectively, field observations support the interpretation of a fluvial depositional environment for the Lower and Middle Siwalik units and an alluvial-fan environment in the Upper Siwalik unit (e.g. Karunakaran and Ranga Rao, 1976; Kumar, 1997; Chirouze et al., 2012). The presence of Himalayan-derived clasts including volcanic rocks observed by us and by Jain et al. (1974) near Likabali suggests some component of basin detritus was derived from the Siang valley during the deposition of the Middle and Upper Siwalik units. The transition from southwest to south-directed paleoflow directions observed from the Middle to Upper Siwalik units may represent transition from deposition in an expansive southwest directed fluvial braidplain (similar to the modern Brahmaputra River) to local deposition by south directed tributaries (e.g. the Subansiri River) and alluvial fans proximal to the mountain front. Alternatively, this change could represent natural variability within an expansive braidplain (Cina et al., 2009) or post-depositional counter-clockwise rotation of these units (Chirouze et al., 2012).

2.2. Provenance constraints from detrital zircon U-Pb geochronology

Single-grain U-Pb dating of detrital zircon cores provides a useful approach to assess sedimentary provenance in the Himalayan foreland basin (e.g., DeCelles et al., 1998; Bernet et al., 2006; Cina et al., 2009). This approach is particularly useful in the eastern Himalayan syntaxis, where published bedrock and detrital ages characterize the range of ages from specific source terranes (e.g. Stewart et al., 2008; Liang et al., 2008; Cina et al., 2009; Zhang et al., 2012; Lang et al., 2013; Robinson et al., 2013). We compiled published datasets from Himalayan and Tibetan source terranes within the eastern syntactical region to constrain the range of ages contributed from each terrane (Fig. 3).

Zircons older than 300 Ma most often represent inherited or detrital grains characteristic of Himalayan and Tibetan units (e.g. DeCelles et al., 2000; Yin et al., 2010; Gehrels et al., 2011; Zhang et al., 2012; Webb et al., 2012), with the important exceptions of some Early Cretaceous-Triassic zircons reported in the Lhasa Terrane (e.g. Leier et al., 2007; Zhu et al., 2011; Li et al., 2013; Lin et al., 2013a), Tethyan Himalaya (e.g. Zhu et al., 2008; Aikman et al., 2008, 2012; Li et al., 2010; Zeng et al., 2011; Webb et al., 2012), and Indus-Tsangpo Suture Zone and adjacent basins (e.g. Wu et al., 2010; Aitchison et al., 2011; Wang et al., 2011; Cai et al., 2012).

Zircons younger than 300 Ma most often represent primary grains from Paleogene-Cretaceous igneous units in Tibet; they may also represent contributions from Neogene-Paleogene igneous units in Tethyan and Greater Himalayan sequences in the Arunachal Himalaya (e.g. Aikman et al., 2008; Hu et al., 2010; McQuarrie et al., 2008; Yin et al., 2010; Zeng et al., 2011; Hou et al., 2012) and Neogene metamorphic units within the vicinity of the Namche Barwa massif (e.g. Ding et al., 2001; Chung et al., 2003, 2009; Booth et al., 2004; Xu et al., 2010, 2012a; Zhang et al., 2010b, 2010c; Guo et al., 2012; Su et al., 2011; Zeng et al., 2012; Lin et al., 2013a; Xu et al., 2013). While these <300 Ma zircons are rare in detrital populations from sediment samples collected in Himalayan tributaries (<5% of the Kameng and Subansiri Rivers, Cina et al., 2009), they dominate sediment samples from Tibetan rivers (Fig. 3).

Multiple source regions contribute <300 Ma zircons from north of the Indus Yarlung Suture Zone in Tibet (Fig. 3). Gangdese plutons and volcanic units west of the Namche Barwa massif yield primarily Paleogene-Late Cretaceous zircons (e.g. Booth et al., 2004; Wen et al., 2008; Zhang et al., 2010a, 2012; Zhu et al., 2011; Guo et al., 2011, 2012; Ji et al., 2012; Guan et al., 2012; Zheng et al., 2012), while Bomi-Chayu igneous sources east of the Namche Barwa massif yield primarily Early Cretaceous zircons (e.g. Booth et al., 2004; Chiu et al., 2009; Liang et al., 2008; Xu et al., 2012b; Zhang et al., 2012; Lin et al., 2013b). Jurassic-Permian zircons are also observed from units in the Nyingchi River headwaters (e.g. Chu et al., 2006; Zhu et al., 2009, 2011; Guo et al., 2011; Zhang et al., 2012; Li et al., 2013; Lin et al., 2013c), and a few published zircon U-Pb analyses from the Lohit Plutonic Suite suggest that this terrane may be a source of Early Cretaceous (Lin et al., 2013b; Haproff et al., 2013) as well as Late Cretaceous zircons (e.g., Lohit River sample of Cina et al., 2009). However, the limited data available for this particular region make this a source of uncertainty in our provenance analysis.

Source region is not the only factor influencing the relative density of detrital zircon U-Pb age probability. For example, age distributions may be strongly influenced by localized, short-term patterns of sediment delivery (e.g. Ruhl and Hodges, 2005; Stock et al., 2006; Avdeev et al., 2011), downstream dilution by contribution from local sources (Zhang et al., 2012), and the heterogeneous distribution of target minerals (i.e. zircon) in source terranes (e.g. Amidon et al., 2005; Duvall et al., 2012). Thus even when a large

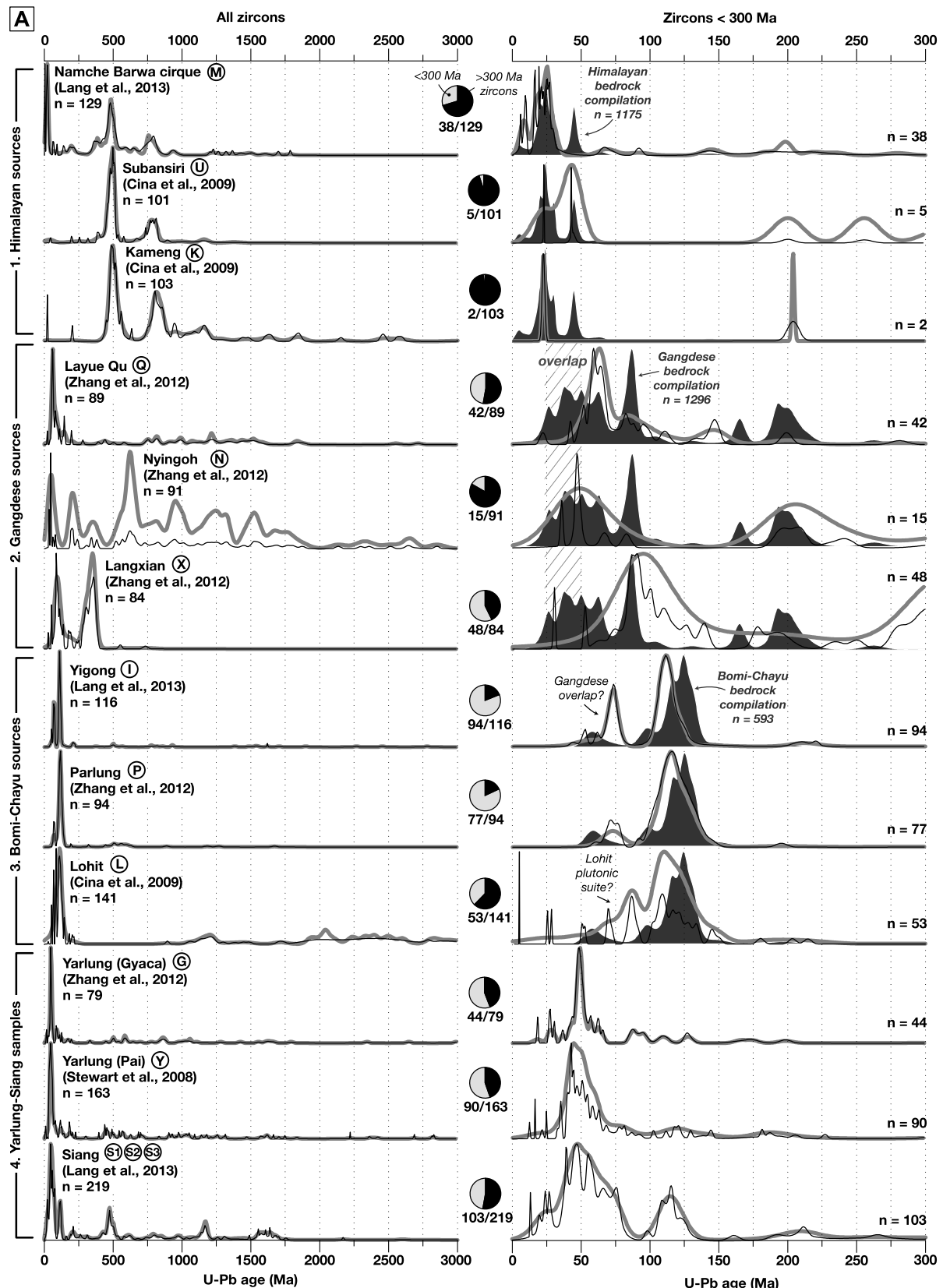


Fig. 3. Compilation of published bedrock and detrital zircon U-Pb ages from the eastern syntaxis region. (A) Compiled age data from 1. Himalaya, 2. Gangdese, 3. Bomi-Chayu sources, and 4. modern samples from the Yarlung and Siang rivers (see text for references). Ages from detrital samples are plotted as normalized summed probability density functions (thin black line) and kernel density estimates (thick gray line). Kernel density estimates are locally adapted to age density with a maximum smoothing bandwidth of 30 Ma (generated using the Density Plotter application of Vermeesch, 2012). Bedrock ages (<300 Ma only) are plotted as solid-dark-gray kernel density estimates for comparison with detrital samples. The full range of observed ages from 0–3000 Ma is shown in the left column, and 0–300 Ma ages are shown in detail in the right column. Pie charts show the fraction of zircons <300 Ma (black) and >300 Ma (white) used in the data compilation in (A).

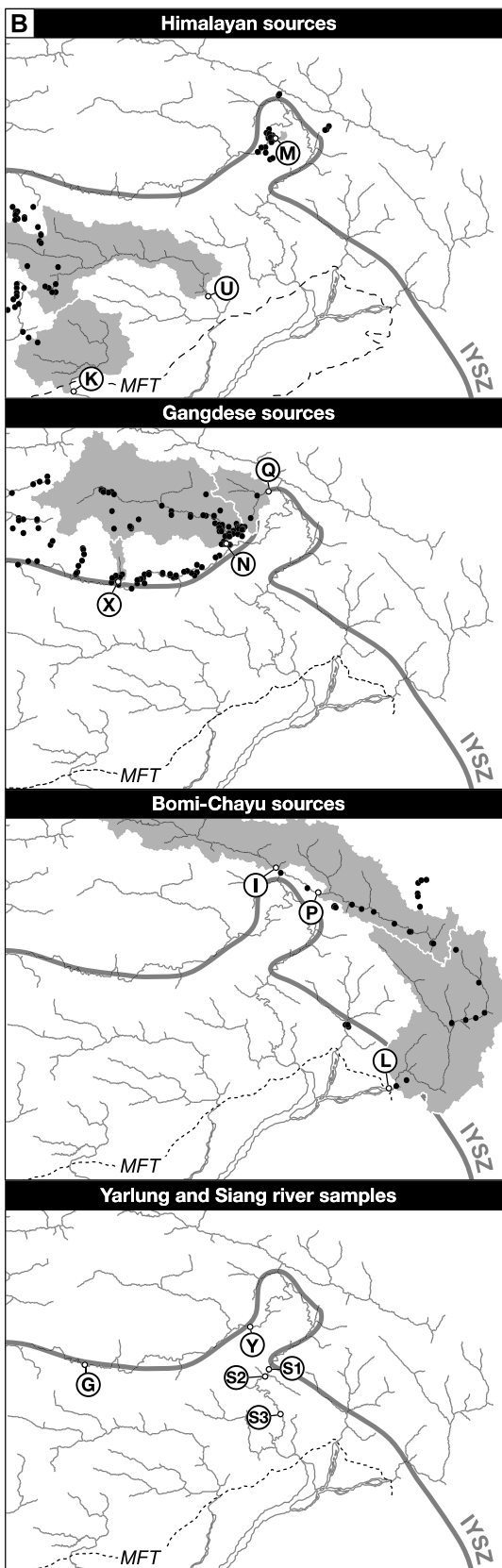


Fig. 3. (continued)

number of detrital grains is analyzed, the absence of a specific age component does not necessarily exclude the possibility that the corresponding source area was within the contributing area of the

sample (Vermeesch, 2004). However, the presence of specific age components is a robust indicator of sedimentary provenance, requiring source terranes to have been within the contributing area of the basin concurrent with or prior to the time of sample deposition. With these considerations, we focus our provenance interpretations on the presence of distinct age components in Siwalik samples.

2.3. Previous constraints on Siwalik provenance in the eastern Himalaya

Coupled detrital zircon U-Pb and ε_{Hf} analyses, as well as bulk ε_{Nd} data constrain Siwalik Group provenance downstream of the modern Subansiri-Brahmaputra River confluence. Cina et al. (2009) have interpreted the presence of Paleogene-Early Cretaceous zircons with ε_{Hf} signatures similar to Gangdese sources as Gangdese detritus in Upper, Middle and Lower Siwalik units. The authors discuss that the presence of this detritus could be explained by either connection of the lower Yarlung River to the Siang River or the upper Yarlung River to the Subansiri River prior to capture by the Siang at some time during deposition of the Middle Siwalik unit, estimated to be before ~ 4 Ma (Clark et al., 2004). They prefer connection of the Yarlung and Subansiri rivers prior to ~ 4 Ma, given additional observations of changing paleoflow directions (from southwest to south) between deposition of the Middle and Upper Siwalik units.

Alternatively, the presence of Gangdese detritus and the change in paleocurrent direction in the Upper Siwaliks could be explained by recycling of Lower and Middle Siwalik units (as observed in the modern Subansiri River samples of Cina et al., 2009). Additional ε_{Nd} isotopic work near Bhalukpong by Chirouze et al. (2013) demonstrates that the Middle Siwalik unit was sourced from a longitudinal river system draining Tibetan sources like the modern Brahmaputra since ~ 7 Ma, but indicates that this source changed to a transverse Himalayan river like the Kameng River during deposition of the Upper Siwalik unit. Pleistocene faulting at the mountain front (Kumar, 1997; Chirouze et al., 2013) would have exposed the Lower and Middle Siwalik units to erosion during deposition of the Upper Siwalik unit, providing an additional source of Gangdese detritus—an interpretation corroborated by evidence of growth strata in the uppermost portion of the Upper Siwalik formation near Bhalukpong (Burgess et al., 2012).

Determining when the Yarlung-Siang River connection was established is important for evaluating explanations for rapid exhumation of the Namche Barwa massif (e.g., initiation in response to rapid, focused river incision following capture of the Yarlung by headward erosion of the Siang). As Cina et al. (2009) point out, if the Yarlung River connected to the Subansiri prior to capture by the Siang ~ 4 Ma, Upper Miocene foreland basin units east of the Subansiri River should not contain Gangdese-age detrital zircons. To test this prediction, we analyzed additional samples from Siwalik units exposed east of the Itanagar section and more proximal to the Siang-Brahmaputra River confluence.

3. Sampling and analytical methods

We collected 15 samples from the three sedimentary sections investigated. The approximate stratigraphic position of each sample is illustrated in Fig. 4. At the section near Likabali we focused on detailing provenance changes with multiple samples from each Siwalik unit, and we evaluated variability of a single unit along strike of the Himalaya with additional Middle Siwalik samples collected near Kimin and Pasighat.

Near Likabali, we sampled compact fine-grained sandstones of the Lower Siwalik unit exposed between the Tipi Thrust and the Main Boundary Thrust. We collected six Middle Siwalik samples

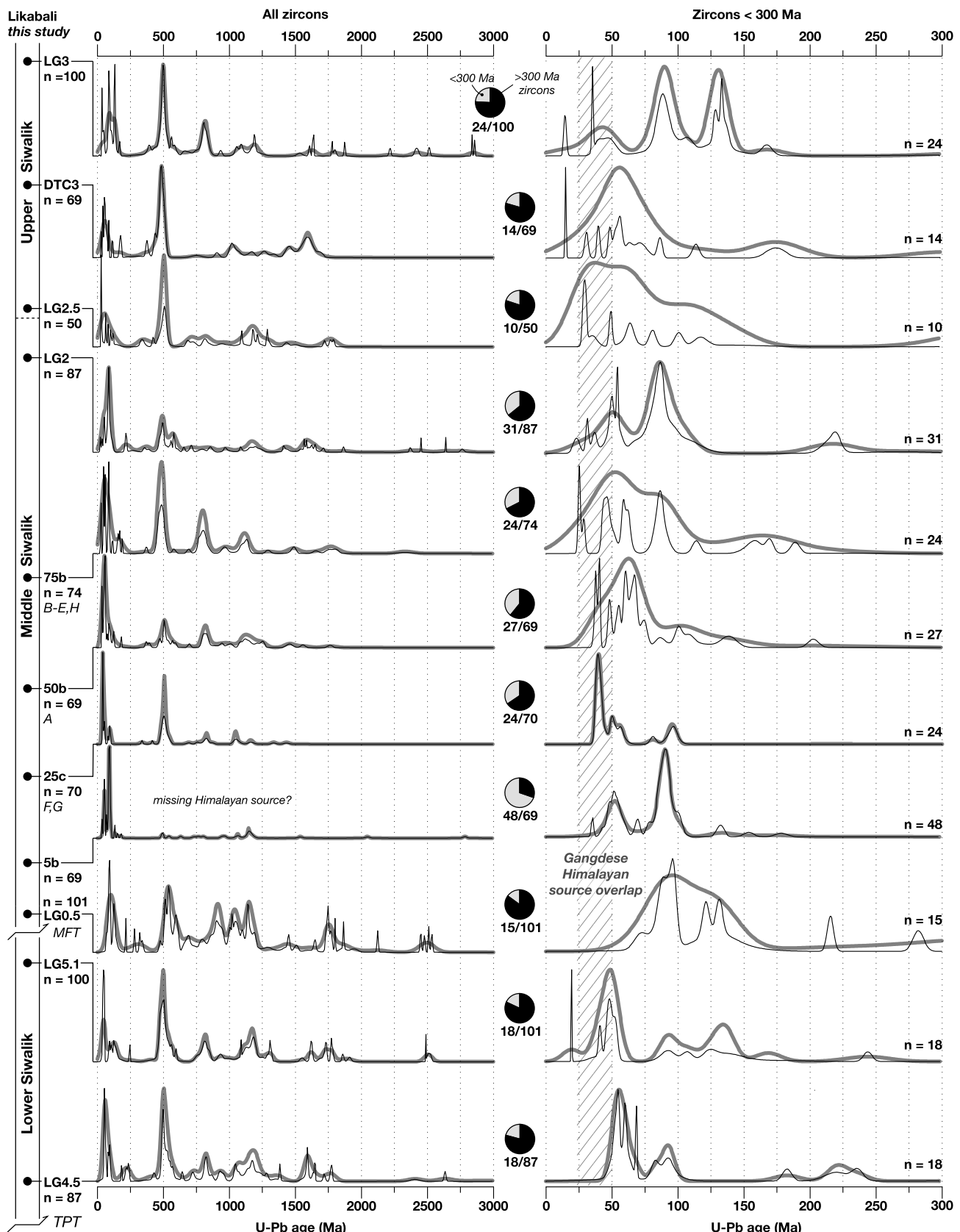


Fig. 4. Detrital zircon U-Pb data from Siwalik units sampled at the three new locations shown in Fig. 1 and data from previously sampled sections at Bhalukpong and Itanagar (Cina et al., 2009) for comparison. Samples are plotted at their approximate stratigraphic position. Paleogene–Late Cretaceous ages characteristic of Gangdese sources west of the Namche Barwa massif are observed in all samples with the exception of the Lower Siwalik unit at Bhalukpong (Cina et al., 2009). Pie charts and age spectra are plotted in the same manner as Fig. 3.

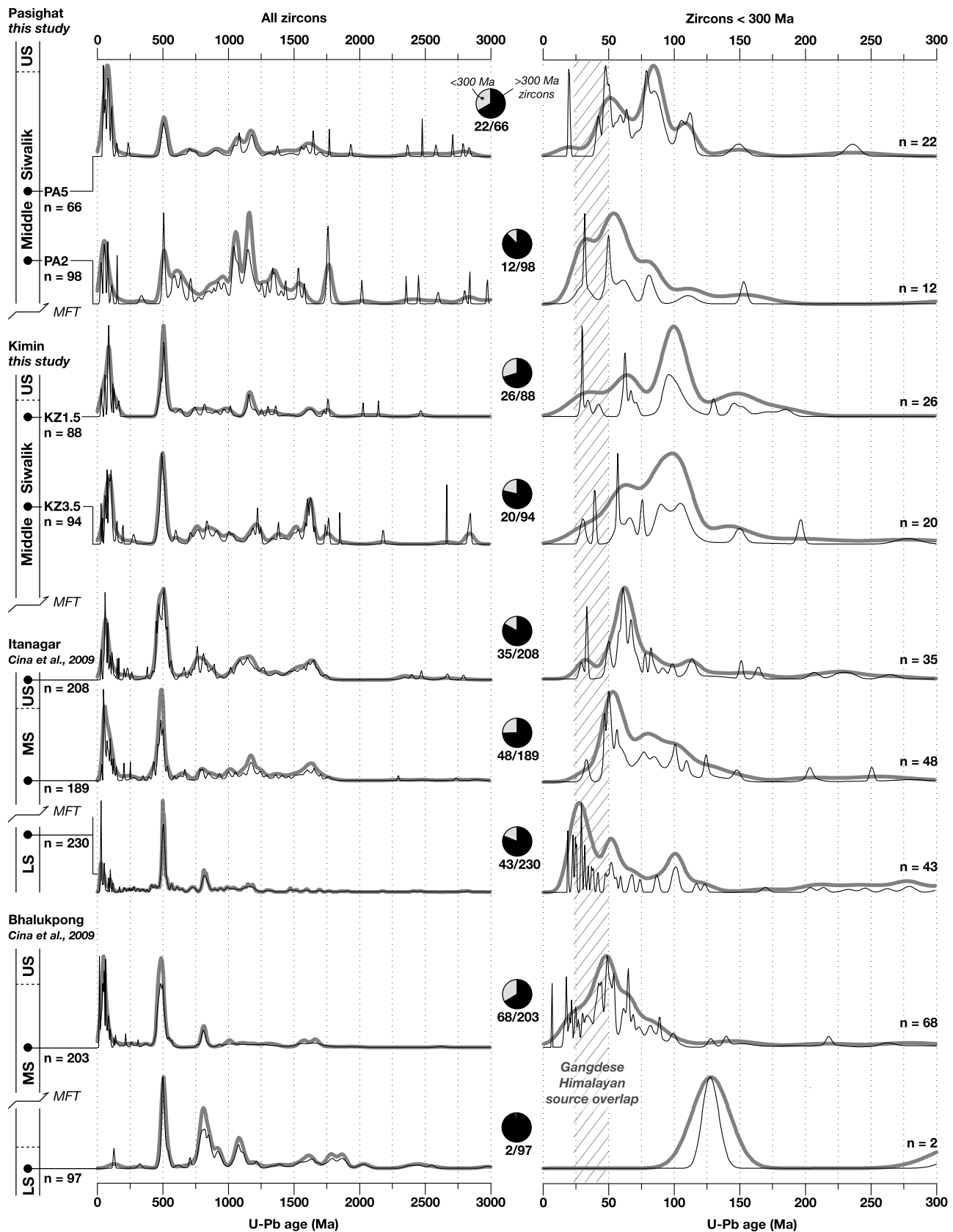


Fig. 4. (continued)

from medium to coarse sandstones exposed along the Siji River and in road exposures, where the unit is uninterrupted by faulting (Jain et al., 1974; Agarwal et al., 1991) between the Main Frontal

Thrust and the conformable Upper-Middle Siwalik contact. We collected three samples from the Upper Siwalik unit including one from a medium sandstone interbedded with siltstone and gravel

conglomerate beds above the Middle Siwalik contact, one from a coarse sandstone interbedded with cobble conglomerate in the middle of the unit, and one from a sand lens within the conspicuous boulder conglomerate at the top of the section near the Tipi Thrust.

Additional Middle Siwalik samples were collected near Kimin and Pasighat from massive medium and coarse sandstones. The two Kimin samples were collected in river exposures between the Tipi Thrust and the Upper-Middle Siwalik contact, and the two Pasighat samples were collected in road exposures along the mountain front.

In preparation for isotopic analysis, sedimentary rock samples were manually disaggregated in a dilute HCl solution and wet sieved to isolate the 63–250 µm size fraction. Zircons were separated from this fraction by standard magnetic and heavy liquid techniques, mounted in epoxy, polished and imaged using high-resolution electron backscatter detection and cathodoluminescence prior to isotopic analysis. U-Th-Pb analyses of a random selection of zircon cores by laser ablation, multicollector inductively coupled plasma mass spectrometry were carried out in two locations: at the University of Arizona LaserChron center and by Apatite to Zircon, Inc. Analyses at the University of Arizona LaserChron center were conducted on a Nu high resolution mass spectrometer coupled to a Photon Machines 193 nm excimer laser with a ~30 µm spot size (Gehrels et al., 2006, 2008). Analyses at Apatite to Zircon, Inc. were conducted on an Agilent 7700× quadrupole mass spectrometer coupled to a Resonetics RESOlution M-50 193 nm excimer laser with a ~30 µm spot size (Donelick et al., 2005; Chew and Donelick, 2012).

We analyzed at least 50 grains per sample (and many more when possible) with the goal of identifying the presence of <300 Ma zircons. Zircons of this age represent ~25% of detrital populations sampled in river sediment near Pasighat (Stewart et al., 2008) and ~10% of detrital populations sampled from Brahmaputra River sediment downstream (Cina et al., 2009); by analyzing 50 grains we can be 95% confident that our analyses did not miss an age component representing >10% of the total (Vermeesch, 2004).

The analytical data and details of standard calibration and isotopic corrections are presented in the Supplementary Material.

4. Results of detrital zircon U-Pb dating and provenance interpretations

A total of 1222 detrital zircon U-Pb analyses produced ages that range from 15 Ma to 3.3 Ga and confirm the presence of a significant component of <300 Ma zircons in each Siwalik unit (Fig. 4). In the section near Likabali, about 20% of zircons in both of the Lower Siwalik samples and in the lowest Middle Siwalik sample are younger than 300 Ma. The three Upper Siwalik samples from this section contain a similar proportion of younger zircons (20–24%). The remaining five samples from this section may suggest an increase in the proportion of <300 Ma zircons during Middle Siwalik deposition—the young zircon population makes up >30% of each sample, and 70% of sample 5b. The additional four Middle Siwalik samples from Pasighat and Kimin are more variable (12–33% young zircons).

In all samples, <300 Ma zircons (333 of the total 1222 grains) are dominantly Paleogene–Late Cretaceous in age, similar to Gangdese bedrock from west of the Namche Barwa massif and detrital zircons from rivers draining that area (Fig. 3). Early Cretaceous zircons characteristic of Bomi–Chayu sources are present in most samples in relatively smaller abundance, with the exception of one Middle Siwalik sample and one Lower Siwalik sample collected near Likabali that lack zircons of this age. Neogene zircons

characteristic of young anatetic units from the Namche Barwa massif are rare.

We interpret the provenance of detrital zircons based on U-Pb age (although complimentary isotopic and modal analysis may further evaluate these interpretations), such that zircons with Paleogene–Late Cretaceous U-Pb ages represent Gangdese detritus and zircons with Early Cretaceous ages represent detritus from a Bomi–Chayu source. Older grains are not as diagnostic, but likely represent Jurassic and Triassic units observed within the Gangdese source area. When observed, Neogene zircons may represent sources in the Arunachal Himalaya or Namche Barwa specifically.

It is possible that some zircons in this age range could come from other sources. Paleogene zircons (specifically ~40–50 Ma) could alternatively represent igneous units in the Tethyan Himalaya; however these rocks are presently exposed over a very small region of the Himalaya and do not represent a significant component of modern Himalayan detrital sediments (e.g., Subansiri and Kameng River samples of Cina et al. (2009) shown in Fig. 3). It is also possible that Paleogene and Cretaceous zircons may represent unobserved sources within the Lohit Plutonic Suite (Early Cretaceous ages in Lohit River sample may be evidence for this), but additional sampling of this region, specifically of the Dibang River drainage, is necessary to confirm this.

Sediment recycling could potentially introduce another source of uncertainty in provenance analysis. Recycling of exposed Siwalik units is an important source of detrital zircons in modern sediment samples (e.g. Cina et al., 2009) and may have been an additional source of zircons once Siwalik units where exhumed along the Himalayan mountain front in the Pleistocene. However, the absence of growth strata in all but the uppermost Upper Siwalik unit indicates that recycling was not likely to be an additional source of zircons until the very end of this depositional sequence, and thus is not a potential source of the zircons observed in Lower and Middle Siwalik units.

5. Discussion

Our results broadly corroborate previous observations of Gangdese detritus within eastern Himalayan foreland basin units (e.g. Cina et al., 2009; Chirouze et al., 2013), and place new constraints on the organization of rivers carrying this detritus into the basin. In particular, we observe Gangdese detritus in samples from the Middle and Lower Siwalik units upstream of the Subansiri–Brahmaputra River confluence, which we propose indicates a connected drainage system from Gangdese sources west of the Namche Barwa massif through the Siang River to the foreland basin at least since deposition of the Lower Siwalik unit began in the Early Miocene. These observations do not exclude the possibility of additional connections from Tibet through the eastern Himalaya during Siwalik deposition, such as between a transverse river like the Subansiri River and the upper ~2/3 of the present Yarlung drainage (Cina et al., 2009). However, an additional connection is not necessary to explain the collective dataset.

5.1. Antecedence of the Yarlung–Siang–Brahmaputra River

The collective detrital zircon U-Pb provenance dataset including the new data presented here, observations from the Siwalik Group sections near Itanagar and Bhalukpong (Cina et al., 2009) and from distal Brahmaputra River deposits (Najman et al., 2008) may be explained by antecedent drainage of the Yarlung–Siang–Brahmaputra River. The Gangdese detritus observed in our Middle and Lower Siwalik samples, as well as the Middle and Lower samples collected near Itanagar and the Middle Siwalik sample collected near Bhalukpong (Fig. 4, Cina et al., 2009) may indicate deposition by

a large southwest flowing river system that connected to the ancestral Yarlung River through the Siang River, a landscape similar to the present. This interpretation is consistent with paleocurrent indicators that indicate deposition of the Middle Siwalik by a southwest flowing river, and connection through the Siang River is further supported by the presence of volcanic clasts in the Middle and Upper Siwalik units.

The presence of Gangdese detritus in Upper Siwalik samples with south-directed paleocurrent indicators has been interpreted to indicate prior connection of the upper Yarlung and Subansiri Rivers (Cina et al., 2009). However, recycled detritus from the Lower and Middle Siwalik units may have been an additional source of zircons during deposition of the Upper Siwalik unit. Thus, south directed paleocurrent indicators in the Upper Siwalik unit could represent local deposition by a south-flowing transverse tributary near the mountain front (e.g. the Subansiri River).

Because the Yarlung River presently follows the Indus Yarlung Suture Zone for over 1000 km prior to entering the Tsango gorge, we speculate that the Yarlung–Siang–Brahmaputra River originally followed a similar eastern course along the suture (Fig. 5A, Brookfield, 1998) after a potential reversal in the Early Miocene (Wang et al., 2013) yet prior to uplift of the Namche Barwa massif. Uplift of the massif progressively warped the suture zone into the distinct U-shape observed today (Fig. 5B), and the river may have followed this warping until it eventually captured and reversed flow of the Parlung River (Fig. 5C; Seward and Burg, 2008).

Although many of the Siwalik samples contain some Early Cretaceous zircons characteristic of Bomi–Chayu sources in addition to the dominant Gangdese component, we argue that this does not suggest that the Gangdese source region was connected to the foreland through the ancestral Parlung and Lohit Rivers. Drainage through the ancestral Parlung and Lohit Rivers would have entrained a larger component of Bomi–Chayu detritus immediately prior to entering the basin, yet Early Cretaceous zircons do not dominate the detrital population. Moreover, although this age range is characteristic of Bomi–Chayu igneous sources, it is also possible that Early Cretaceous zircons originated from unobserved northern igneous sources (e.g. the northern igneous belt of Zhang et al., 2012), and thus their presence does not demand routing of Gangdese detritus through the Lohit drainage. Rather, the dominance of Gangdese detritus in every sample we measured suggests that at least during deposition of the Middle and Lower Siwalik units, a river carried Gangdese detritus directly to the basin avoiding a more circuitous route through the ancestral Parlung and Lohit Rivers.

Observations of Gangdese detritus in Burmese basins (Robinson et al., 2013) require drainage from Gangdese sources into Burma prior to ~18 Ma. We propose that a separate, integrated Yigong–Parlung–Irrawaddy river may explain these observations until an Early Miocene capture event rerouted flow into the Lohit River (e.g. Clark et al., 2004; Robinson et al., 2013). The absence of Bomi–Chayu detritus in the lowest Lower Siwalik sample at Likabali may be consistent with this drainage configuration prior to capture by the Lohit, but additional analyses are necessary from the lowest Siwalik strata to confirm this.

5.2. Capture and reversal of the Parlung River

The geomorphic evidence for reversal of the Parlung River may be explained by capture of the ancestral Yigong–Parlung–Lohit River as lateral propagation of the Namche Barwa massif forced the Yarlung–Siang–Brahmaputra northward (Seward and Burg, 2008). Capture of the Yigong and Parlung drainage areas would have added Early Cretaceous zircons with a characteristic Bomi–Chayu provenance to the Yarlung–Siang–Brahmaputra sediment load, as is presently observed in modern river sediment sampled from

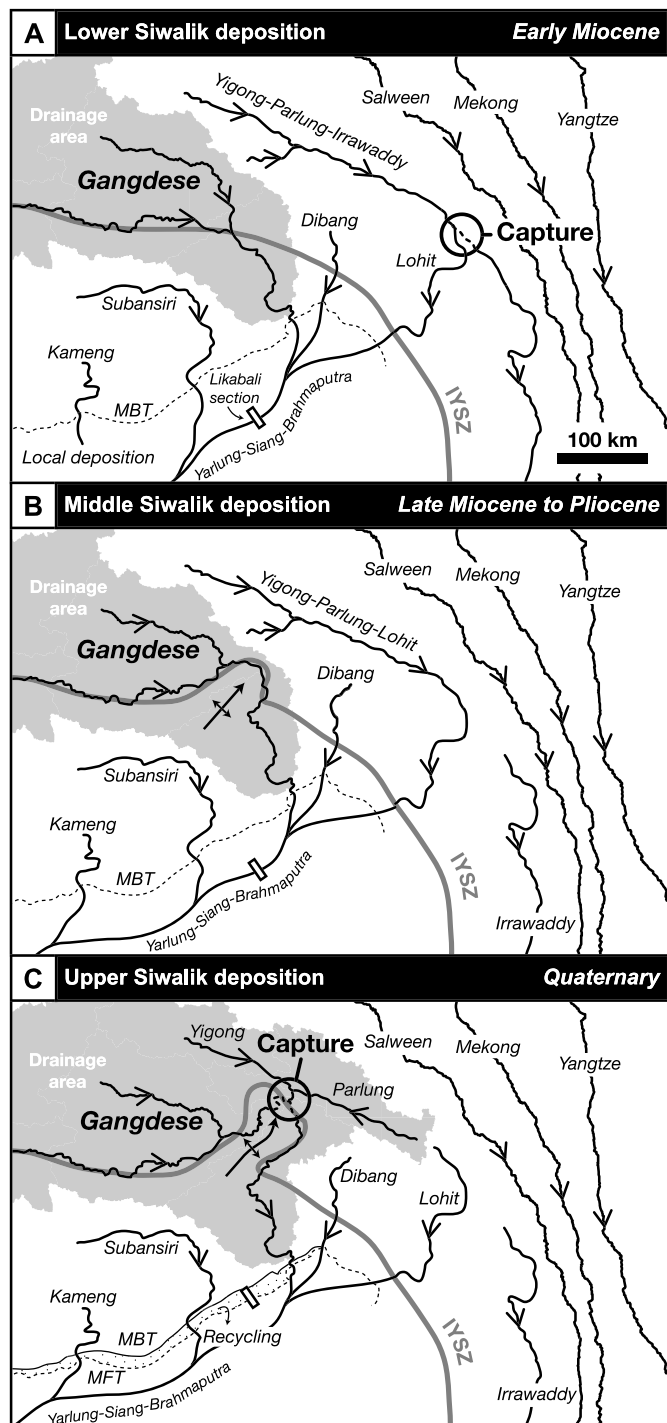


Fig. 5. Proposed drainage evolution of rivers flowing into the eastern Himalayan foreland basin. (A) Connection of the Yarlung–Siang–Brahmaputra River was established during or prior to deposition of the Lower Siwalik unit in the Early Miocene. The ancestral Yarlung River may have followed the IYSZ into the basin as an ancestral Yigong–Parlung River connected to the Irrawaddy system prior to capture by the Lohit River at ~18 Ma (Robinson et al., 2013). (B) Uplift of the Namche Barwa massif began to warp the IYSZ into a U-shape, steepening the Yarlung–Siang–Brahmaputra where it crosses the structure and initiating rapid exhumation of the massif. (C) Lateral propagation of the massif eventually led to capture of the Yigong and Parlung Rivers, reversing flow of the Parlung. The timing of this event remains poorly constrained but may have been influenced by glacial activity in the Quaternary Period.

the Siang River upstream of Siwalik exposures (see Fig. 3). If this capture occurred in the Quaternary (Fig. 5C), potentially influenced by glacial activity (e.g. drainage divide retreat – Oskin

and Burbank, 2005; or temporary damming – Riedel et al., 2007; Korup and Montgomery, 2010), we might expect an increase of Early Cretaceous zircons in the uppermost Upper Siwalik unit. Our youngest sample collected near Likabali may be consistent with this prediction, but does not permit us to test this hypothesis due to the potential influence of sedimentary recycling and low number of analyses. Additional, and more detailed provenance analyses of the proximal Upper Siwalik samples and Late Quaternary terraces (e.g. Srivastava et al., 2008) near the Siang River confluence may further test this hypothesis to constrain the timing of capture and reversal of the Parlung River.

5.3. Exhumation of the Namche Barwa massif

Rapid exhumation of the Namche Barwa massif is estimated to have initiated in the Pliocene or Late Miocene. We propose that integration of the Yarlung–Siang–Brahmaputra river was established by at least the Early Miocene, which implies that rapid exhumation did not initiate in response to capture of the ancestral Yarlung River by headward erosion of the Siang. Instead, antecedence of the Yarlung–Siang–Brahmaputra River demonstrates the potential for the progressive coevolution of rapid rock uplift and erosion of the Namche Barwa massif. Fluvial incision may amplify crustal deformation in the presence of regional compressive stresses (Simpson, 2004) as has been previously observed along Himalayan river anticlines (e.g. Montgomery and Stolar, 2006). We propose that coincident rock uplift associated with folding of the Namche Barwa antiform and erosion in the antecedent river channel locally increased exhumation rates at the margin of the Tibetan plateau without requiring a dramatic increase in drainage area. Sustained exhumation of the plateau margin, perhaps further increased after capture of the Yigong and Parlung Rivers, may have eventually removed enough crustal material to develop a thermo-mechanical feedback producing high topography over hot, weak crust (e.g. Zeitler et al., 2001; Koons et al., 2013).

6. Conclusions

We used detrital zircon U–Pb geochronology to determine the sedimentary provenance of Siwalik units exposed in three new locations in the eastern Himalayan foreland basin proximal to where the Yarlung–Siang–Brahmaputra River enters the basin. We observe a significant component of young, Paleogene–Late Cretaceous detrital zircons in all samples throughout the sedimentary sequence and interpret these ages to represent detritus from Gangdese source rocks west of the Namche Barwa massif. These results corroborate previous observations of Gangdese-age detritus within the eastern Himalayan foreland basin and further suggest that connection of the Yarlung–Siang–Brahmaputra River was established by the time deposition of the Lower Siwalik unit began in the Early Miocene. Rapid exhumation of the Namche Barwa massif is thought to have initiated later, in the Pliocene or Late Miocene, and therefore we propose that exhumation of the massif was not related to capture of an ancestral Yarlung River by headward erosion of the Siang River. Considering this, we prefer the explanation for reversal of the Parlung River via capture by an integrated Yarlung–Siang–Brahmaputra as the rivers were tectonically juxtaposed by lateral propagation of the Namche Barwa massif. Antecedence of the Yarlung–Siang–Brahmaputra River demonstrates the potential for the progressive coevolution of rock uplift, and fluvial incision of the Namche Barwa massif, such that sustained erosion at the plateau margin may have eventually initiated a thermo-mechanical feedback that focused crustal exhumation in the region.

Acknowledgements

The authors acknowledge funding from the National Science Foundation (NSF-EAR 1349279 and NSF-EAR 0955309 to K.W.H., NSF-EAR 1032156 for support of the Arizona LaserChron Center), the Geological Society of America (Graduate Student Research Grant to K.A.L.), and the Quaternary Research Center at the University of Washington. The authors thank V. Adlakha, K. Bage and O. Tayeng for field assistance, K. Atatürk and K. Sumner for laboratory assistance, and T.M. Harrison for editorial support. This paper greatly benefited from detailed reviews from E. Garzanti, D. Burbank and A. Yin as well as informal reviews and comments by D. Montgomery and B. Hallet.

Appendix A. Supplementary material

Supplementary material related to this article can be found online at <http://dx.doi.org/10.1016/j.epsl.2014.04.026>.

References

- Acharya, S.K., 2007. Evolution of the Himalayan Paleogene foreland basin, influence of its litho-packet on the formation of thrust-related domes and windows in the Eastern Himalayas – a review. *J. Geol. Soc. India* 31, 1–17.
- Agarwal, R.P., Srivastava, Maithani A, A.K., 1991. Geology of the Eastern Himalayan foothill belt of Bhutan and Arunachal Pradesh: an overview. *J. Himal. Geol.* 2 (2), 197–205.
- Aikman, A.B., Harrison, T.M., Lin, D., 2008. Evidence for Early (>44 Ma) Himalayan crustal thickening, tethyan Himalaya, southeastern Tibet. *Earth Planet. Sci. Lett.* 274 (1–2), 14–23.
- Aikman, A.B., Harrison, T.M., Hermann, J., 2012. The origin of Eo- and Neo-Himalayan granitoids, Eastern Tibet. *J. Asian Earth Sci.* 58, 143–157.
- Aitchison, J.C., Xia, X., Baxter, A.T., Ali, J.R., 2011. Detrital zircon U–Pb ages along the Yarlung–Tsangpo suture zone, Tibet: implications for oblique convergence and collision between India and Asia. *Gondwana Res.* 20, 691–709.
- Ali, J.R., Aitchison, J.C., Chik, S.Y.S., Baxter, A.T., Bryan, S.E., 2012. Paleomagnetic data support Early Permian age for the Abor Volcanics in the lower Siang Valley, NE India: significance for Gondwana-related break-up models. *J. Asian Earth Sci.* 50, 105–115.
- Amidon, W.H., Burbank, D.W., Gehrels, G.E., 2005. Construction of detrital mineral populations: insights from mixing of U–Pb zircon ages in Himalayan rivers. *Basin Res.* 17 (4), 463–485.
- Armijo, R., Tapponnier, P., Han, T., 1989. Late cenozoic right-lateral strike-slip faulting in Southern Tibet. *J. Geophys. Res.* 94 (B3), 2787–2838.
- Avdeev, B., Niemi, N.A., Clark, M.K., 2011. Doing more with less: Bayesian estimation of erosion models with detrital thermochronometric data. *Earth Planet. Sci. Lett.* 305 (3–4), 385–395.
- Bernet, M., van der Beek, P., Pik, R., Huyghe, P., Mugnier, J.-L., Labrin, E., Szulc, A., 2006. Miocene to recent exhumation of the central Himalaya determined from combined detrital zircon fission-track and U/Pb analysis of Siwalik sediments, western Nepal. *Basin Res.* 18, 393–412.
- Booth, A.L., Zeitler, P.K., Kidd, W.S.F., Wooden, J., Lui, Y., Idleman, B., Hren, M., Chamberlain, C.P., 2004. U–Pb zircon constraints on the tectonic evolution of southeastern Tibet, Namche Barwa area. *Am. J. Sci.* 304, 889–929.
- Booth, A.L., Chamberlain, C.P., Kidd, W.S.F., Zeitler, P.K., 2009. Constraints on the metamorphic evolution of the eastern Himalayan syntaxis from geochronologic and petrologic studies of Namche Barwa. *Geol. Soc. Am. Bull.* 121, 385–407.
- Brookfield, M.E., 1998. The evolution of the great river systems of southern Asia during the Cenozoic India–Asia collision: rivers draining southwards. *Geomorphology* 22, 285–312.
- Burchfiel, B.C., Clark, M.K., Wang, E., Chen, Z., Liu Pan G, Y., 2000. Tectonic framework of the Namche Barwa region, eastern Himalayan syntaxis, SE Tibet. *Abstr. Programs – Geol. Soc. Am.* 32, A-33.
- Burg, J.-P., Podladchikov, Y., 1999. Lithospheric scale folding: numerical modeling and application to the Himalayan syntaxes. *Int. J. Earth Sci.* 88, 190–200.
- Burg, J.-P., Davy, P., Nievergelt, P., Oberli, F., Seward, D., Diao, Z., Meier, M., 1997. Exhumation during folding in the Namche Barwa syntaxis. *Terra Nova* 9, 53–56.
- Burg, J.-P., Nievergelt, P., Oberli, F., Seward, D., Davy, P., Mauring, J.-C., Diao, Z., Meier, M., 1998. The Namche Barwa syntaxis: evidence for exhumation related to compressional crustal folding. *J. Asian Earth Sci.* 16, 239–252.
- Burgess, W.P., Yin, A., Dubey, C.S., Shen, Z.K., Kelty, T.K., 2012. Holocene shortening across the Main Frontal Thrust zone in the eastern Himalaya. *Earth Planet. Sci. Lett.* 357–358, 152–167.
- Burrard, S.G., Hayden, H.H., 1907. *Geography and Geology of Himalayan Mountains and Tibet, Part 3: The Rivers of Himalaya and Tibet*. Government of India Press, Calcutta, pp. 119–230.

- Zhang, H.-F., Harris, N., Guo, L., Xu, W., 2010c. The significance of Cenozoic magmatism from the western margin of the eastern syntaxis, southeast Tibet. *Contrib. Mineral. Petrol.* 160, 83–98.
- Zhang, J.Y., Yin, A., Liu, W.C., Wu, F.Y., Lin, D., Grove, M., 2012. Coupled U-Pb dating and Hf isotopic analysis of detrital zircon of modern river sand from the Yalu River (Yarlung Tsangpo) drainage system in southern Tibet: constraints on the transport processes and evolution of Himalayan rivers. *Geol. Soc. Am. Bull.* 124, 1449–1473.
- Zheng, Y.-C., Hou, Z.-Q., Li, Q.-Y., Sun, Q.-Z., Liang, W., Fu, Q., Li, W., Huang, K.-X., 2012. Origin of Late Oligocene adakitic intrusives in the southeastern Lhasa terrane: evidence from in situ zircon U-Pb dating, Hf-O isotopes, and whole rock geochemistry. *Lithos* 148, 296–311.
- Zhu, D.-C., Mo, Y.-X., Pan, G.-T., Zhao, Z., Dong, G.-C., Shi, Y., Liao, Z., Wang, L.-Q., Zhou, C.-Y., 2008. Petrogenesis of the earliest Early Cretaceous mafic rocks from the Cona area of the eastern Tethyan Himalaya in South Tibet: interaction between the incubating Kerguelen plume and the eastern Greater India Lithosphere? *Lithos* 100 (1–4), 147–173.
- Zhu, D.-C., Mo, X.-X., Niu, Y., Zhao, Z.-D., Wang, L.-Q., Pan, G.-T., Wu, F.-Y., 2009. Zircon U-Pb dating and in-situ Hf isotopic analysis of Permian peraluminous granite in the Lhasa terrane, southern Tibet: implications for Permian collisional orogeny and paleogeography. *Tectonophysics* 469, 48–60.
- Zhu, D.-C., Zhao, Z.-D., Niu, Y., Mo, X.-X., Chung, S.-L., Hou, Z.-Q., Wang, L.-Q., Wu, F.-Y., 2011. The Lhasa terrane: record of a microcontinent and its histories of drift and growth. *Earth Planet. Sci. Lett.* 301, 241–255.